EFFECTS OF CHANNEL GEOMETRY AND COOLANT FLUID ON THERMOELECTRIC NET POWER

A. Rezania[1], L.A. Rosendahl, K. Sørensen

Department of Energy Technology, Aalborg University, DK-9220 Aalborg, Denmark

[1]Corresponding author, E-mail:alr@et.aau.dk

ABSTRACT

Channel geometry has a strong influence on the heat transfer coefficient and cooling energy input in a heat sink. The net power output in a thermoelectric generator (TEG) can be defined as power generation minus the required cooling energy in TEG. This study aims to evaluate the net power generation in TEG for different size of hydraulic diameter of plate-fin heat sink and over a wide range of Reynolds number. The particular focus of this study is to find optimal Reynolds number in each considered channel hydraulic diameter and to explore optimal channel hydraulic diameter for maximum TEG net power output. Three-dimensional governing equations for the flow and the heat transfer and thermal-electrics are solved using the computational fluid dynamics (CFD) simulation environment. The results show that there is an optimal Reynolds number that provides maximum net power output in the TEG, and the maximum net power output occurs at smaller Reynolds number when the channel hydraulic diameter reduces.

KEYWORDS: Thermoelectric generator, plate-fin heat sink, geometry effect, net power.

1. INTRODUCTION

Micro-structured heat sinks provide compact and low weight energy system and can enhance modularity of power systems. This type of heat sink has been interesting for researchers in field of waste heat recovery applications such as thermoelectric generators (TEGs) [1, 2]. TEGs convert heat energy to electrical power by means of semiconductor charge carriers due to temperature difference between a heat source and a heat sink. A key factor in TEG application is to design an optimal heat sink to enhance the power generation in the TEG. Heat transfer coefficient provided by the heat sink critically affects temperature distribution in the thermoelements and their optimum dimensions design for maximum power generation by the TEG [3]. Thermoelements with different temperature distribution generate different electric voltage. Therefore, the impact of the heat sink geometry on flow and temperature distribution needs to be carefully considered to create high heat transfer coefficient in the heat sink [4, 5].

NOMENCLATURE

A	area, m^2
D_h	hydraulic diameter, m
c	specific heat capacity, $\mathrm{J/kg.K}$
H	channel height , m
J	electric current density, $\mathrm{A/m^2}$
k	thermal conductivity, $\mathrm{W/m.K}$
N	number of channels in heat sink
Nu	Nusselt number
P	power, W
p	pressure, Pa
q	heat flux across TEG, $\mathrm{W/m^2}$
$\dot{q}$	heat generation rate per unit volume, $\mathrm{W/m^3}$
R	internal electrical resistance, Ω
Re	Reynolds number
T	temperature, K
ΔT	temperature difference, K
$\vec{V}$	velocity vector, $\mathrm{m/s}$
v	velocity, $\mathrm{m/s}$
W	volumetric flow rate, $\mathrm{m^3/s}$
w	channel width, m

Greek symbols

α	Seebeck coefficient, $\mathrm{V/K}$
μ	dynamic viscosity, $\mathrm{N.s/m^2}$
Π	Peltier coefficient, V
ρ	fluid density, $\mathrm{kg/m^3}$
σ	electrical conductivity, $\mathrm{S/m}$
φ	electric scalar potential, V

Subscripts

c	cooling energy
cr	ceramic
f	coolant fluid
n	n-type thermoelement
net	net
max	maximum
p	p-type thermoelement
ce	cooling energy
w	wall

The voltage generation due to temperature difference of the hot and cold junctions of TEG can be improved by reduction of thermal resistance in heat sink. Because the performance of TEG system also depends on required cooling energy [6, 7], pressure drop is an important factor beside the thermal resistance consideration for optimization of heat sink design. One way to reduce the thermal resistance is to increase mass flow rate in channels of heat sink. However, a higher cooling energy input is required for a given channel hydraulic diameter because of rapidly increase of the pressure drop in the channels. Depending to TEG operating temperature, this cooling energy input can be higher than the power generation by TEG module and cause to negative net power (power generation by the TEG minus required cooling energy input in the heat sink) by the module [8]. Moreover, heat transfer in the heat sink enhances when the channel hydraulic diameter decreases at constant Reynolds number and channels ratio. Smaller channel hydraulic diameter causes lower heat sink thermal resistance. The channel ratio is defined as ration of the channel height to the channel width. Smaller hydraulic diameter also causes higher pressure drop in the channels that increases the coolant energy input in the heat sink.

Rectangular cross-section shaped channels have highest heat transfer coefficient amongst trapezoidal and triangular shaped microchannels [9]. In addition, it gives minimum thermal resistance when the channel width and the fin thickness are equal [10]. Jang et al. [11] explored optimal fin height and number of fins in rectangular channel heat sink to maximize the net power density in TEGs. The results that provide useful information for waste heat recovery applications, suggest proper flue gas velocity for maximum net power output of TEG per the heat sink base area.

In this study, the effectiveness of compact micro-structured heat sink on the power generation and cooling energy input is considered to maximize net power output in TEG. The optimal range of channel hydraulic diameter is explored over practical range of Reynold number to find maximum net power output. In order to reduce thermal resistance of the heat sink and to provide compact heat sinks, the microchannels are designed on the cold side

ceramic layers of TEG module. There are four types of heat sinks in this study. The fluid and thermal characteristics in the heat sinks are considered in laminar regime.

2. GOVERNING EQUATIONS

The coupled thermoelectric constitutive equations (heat flow and the continuity of electric charge) under steady-state condition are defined as follow [12]:

$$\nabla.([\Pi].J) - \nabla.\left([k_{\mathrm{teg}}].\nabla T\right) = \dot{q}, \tag{1}$$

$$\nabla.([\sigma].[\alpha].\nabla T) + \nabla.([\sigma].\nabla\varphi) = 0. \tag{2}$$

The maximum power generation in the TEG, where the internal electrical resistance of the uni-couple is equal to the imposed electrical load resistance, is:

$$P_{\max} = \frac{(\alpha\Delta T)^2}{4R}. \tag{3}$$

where the internal resistance of TEG module is total electrical resistance of the n-type and p-type thermocouples [13]:

$$R = n \times \left(R_{\mathrm{n}} + R_{\mathrm{p}}\right) = n \times \left[\left(\sigma_{\mathrm{n}}\frac{A_{\mathrm{n}}}{H_{\mathrm{n}}}\right)^{-1} + \left(\sigma_{\mathrm{p}}\frac{A_{\mathrm{p}}}{H_{\mathrm{p}}}\right)^{-1}\right]. \tag{4}$$

The length and width of the TEG module are $7.2\,\mathrm{mm}$, and the height of thermoelements in this studied is $1.4\,\mathrm{mm}$ with squared footprint area equal to $1\,\mathrm{mm}^2$. The distance between the thermoelements is $0.8\,\mathrm{mm}$. The interconnectors that connect the thermoelements to each other are silver with thermal conductivity of $429\,\mathrm{W/K.m}$, and its electric resistivity varies with $0.0038\mathrm{T} + 1.52 \times 10^{-8}\,\Omega.\mathrm{m}$ [14]. The applied thermoelectric material is Bismuth Telluride ($\mathrm{Bi_2Te_3}$) with thermal conductivity, electrical resistivity and Seebeck coefficient equal to $1.2\,\mathrm{W/m.K}$, $9.09\,\Omega.\mathrm{m}$ and $\pm 0.2\ \mathrm{mV/K}$, respectively.

Equations (5), (6) and (7) represent continuity, momentum and energy in the heat sink under laminar and incompressible flow conditions [15]:

$$\nabla.\vec{V} = 0, \tag{5}$$

$$\rho_{\mathrm{f}}\left(\vec{V}\nabla.\vec{V}\right) = -\nabla p + \mu_{\mathrm{f}}\nabla^2\vec{V}, \tag{6}$$

$$\rho_{\mathrm{f}}c_{\mathrm{f}}\left(\vec{V}.\nabla T\right) = k_{\mathrm{f}}\nabla^2 T. \tag{7}$$

As mentioned, pressure drop in heat sink is an important factor that influences net power of the TEG module. Required cooling energy is related to the pressure drop and the volumetric flow rate in the heat sink:

$$P_{\mathrm{ce}} = \Delta p W. \tag{8}$$

The net power output of the TEG is defined as follows:

$$P_{\mathrm{net}} = P_{\mathrm{teg}} - P_{\mathrm{ce}}. \tag{9}$$

Water is used as the coolant fluid in this study with inlet temperature of $290\,\mathrm{K}$. Range of the Reynolds number in the microchannels is $2 - 2000$, and the hot junction temperature of TEG is fixed at $400\,\mathrm{K}$. Table 1 presents properties of the coolant fluid and the heat sink used in the simulation. Hydraulic diameter of the designed channels in heat sinks N4, N8, N24 and N72 are $900\,\mu\mathrm{m}$, $450\,\mu\mathrm{m}$, $150\,\mu\mathrm{m}$ and $50\,\mu\mathrm{m}$, respectively, where N represents number of microchannels in heat sink. The channels dimensions (width and height) and the fin thickness are considered equal. Fig. 1 shows configuration of the heat sinks with the TEG. The thermoelectrical characteristics of the thermoelements are

implemented in a three dimensional simulation environment and are solved by the finite element method, Mechanical, in conjunction with the computational fluid dynamics (CFD) simulation environment, CFX, that solve the coupled thermal and fluid equations in the heat sinks and coolant fluid.

Table 1 Properties of the coolant fluid and the heat sink.

Dimension	k_{cr}(W/m K)	k_f(W/m K)	ρ_f(kg/m^3)
Value	30	0.6	998.2
Dimension	μ_f(kg/m. s)	c_f(J/kg. K)	
Value	0.001	4182	

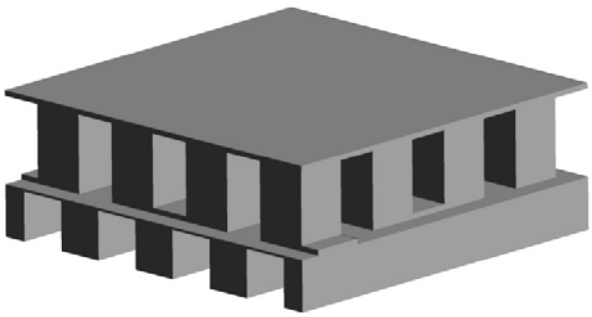

a.

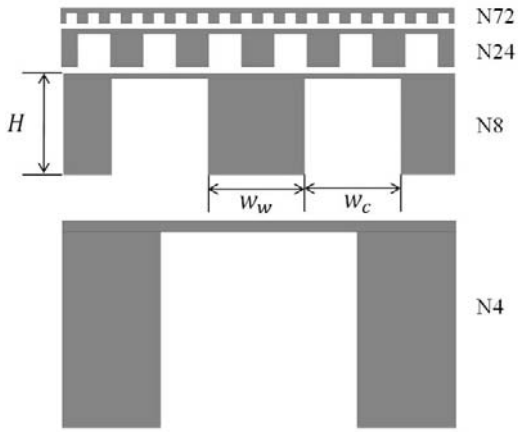

b.

Fig. 1 **a.** Configuration of the studied TEG **b.** front view of symmetric domain of studied heat sinks (A quarter of heat sink geometry is shown here for better resolution).

3. RESULTS

Thermal characteristic of the microchannels in this study is validated with [16] with the same geometrical details. Fig. 2 shows variation of the circumferential Nusselt number along the channel with the same boundary conditions that are is in good agreement with previous study.

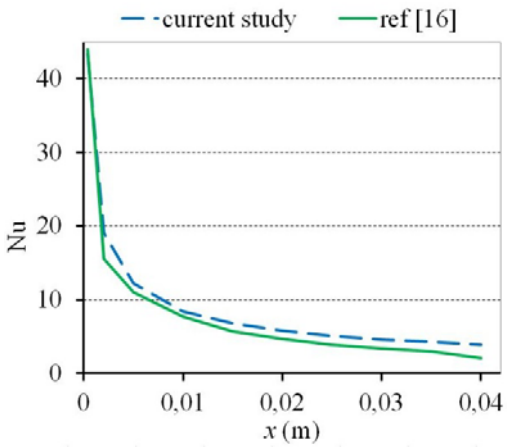

Fig. 2 Comparison of Nusselt number in the microchannel with ref [31] ($H_c = 500$ µm, $w_c = 300$ µm $v_i = 3$ m/s $T_i = 293.15$ K, $q = 30$ W/cm^2).

The computational model used in this study is able to demonstrate 3D results of temperature distribution and voltage generation in the TEG affected by the flow in the micro-structured heat sinks. As Fig. 3 shows, temperature of the flow rises along the channels because of heat absorbed from the TEG. Therefore, temperature on the cold junction of the thermoelements is not constant, and each thermoelement generates different electric voltage. Fig. 4 illustrates how electrical potential increases in the series design of n and p-type thermoelement.

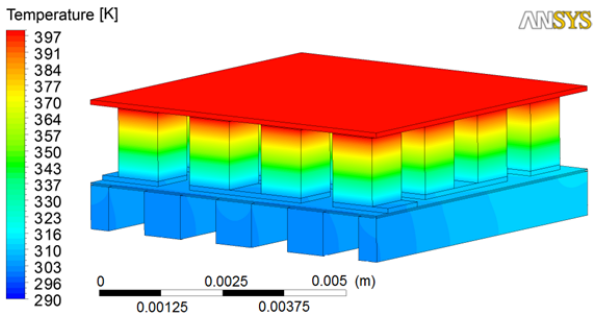

Fig. 3 Temperature distribution in the TEG and fins of heat sink. Re = 10.

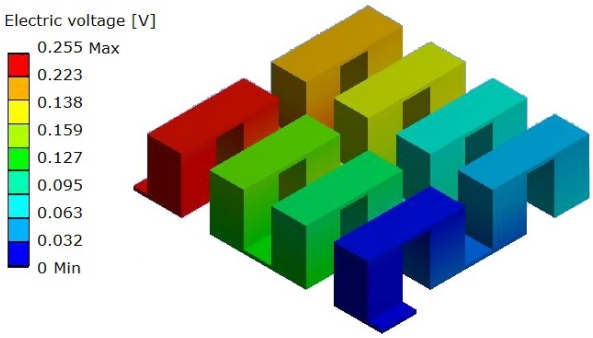

Fig. 4 Generation of the electric voltage in TEG. R = 10.

The results show that, when the hydraulic diameter of channels decreases, the maximum net power output happens at lower Reynolds number. For a given Reynolds number in the channels and constant hot junction temperature on the TEG, the thermal resistance of the heat sink decreases with the channel hydraulic diameter. The smaller thermal resistance provides lower temperature at the cold junction of the TEG module and increases voltage generation in the TEG. On the other hand, pressure drop in the channel increases at smaller channel and causes higher cooling energy input. This elevation of pressure drop is rapid at high Reynolds number condition, and creates significant cooling energy required in the heat sink, as shown in Fig. 5.

To avoid of evaporation of water due to absorbing of heat in the channels, the minimum Reynolds number considered in this study is Re = 2. However, since water has high specific heat capacity, suitable temperature can be achieved on the TEG cold junction at low Reynolds numbers. The cold junction of TEG remains at close temperature to the flow inlet temperature and thermal resistance of the heat sink is small under high Reynolds number conditions. Therefore, power generation in the TEG increase slightly with the Reynolds number compared to the low Reynolds number conditions. In this case, specifically when the channels have small hydraulic diameter, the net power of the system can be negative because of high cooling energy in the heat sink. Depending to the hydraulic diameter of the micro-channels, the limitation of Reynolds number needs to be carefully considered to avoid negative net power output. There is an optimal value for the Reynolds number for each design of heat sink that the net power output is at maximum value. This optimal Reynolds number is lower when the hydraulic diameter of channels is smaller. For example, the optimal Reynolds number for studied heat sinks N72, N24, N8 and N4 are Re = 50, Re = 200, Re = 500 and Re = 100, respectively.

For a given TEG design and its hot junction temperature and for constant thermoelectric material properties, a higher heat flux across the TEG means a higher temperature different between the cold and hot junctions of the TEG. Since the power generation depends to this temperature difference according to (3), if the heat flux enhances the voltage generation in the TEG increases. Fig. 6 shows how the maximum power generation in TEG follows the heat flux across the TEGs.

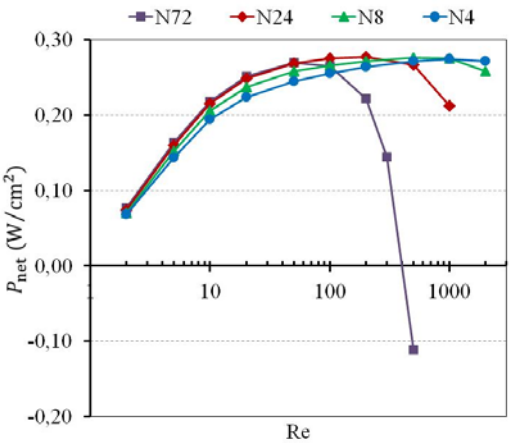

Fig. 5 Variation of TEG net power output with variation of Reynolds number in channels.

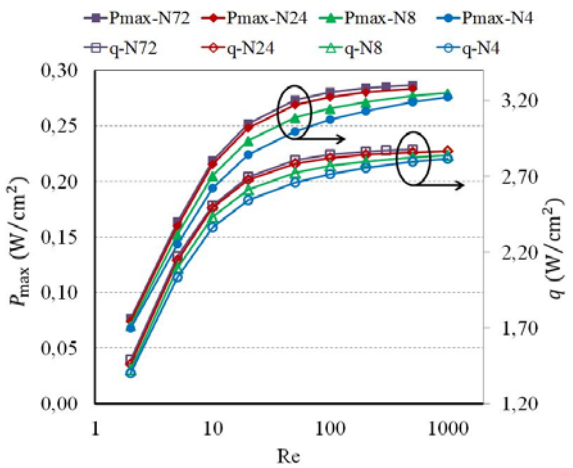

Fig. 6 Variation of thermoelectric maximum power generation and heat flux across the TEG with variation of Reynolds number.

4. CONCLUSIONS

In this study, effect of hydraulic diameter of microchannels on the power generation and net power output in TEGs and cooling energy input in heat sink is considered over a wide range of Reynolds number. The 3D governing equations of thermoelectricity and flow are solved, and analysis of the model generated detailed description of the temperature distribution and voltage generation in the TEGs and heat sinks. The results of this study show that there is an optimal Reynolds number of flow in each heat sink that provides maximum net power output in the TEG. The maximum net power output occurs at smaller Reynolds number when the channel hydraulic diameter reduces. As future work, the results will be developed with consideration of other channel cross section shapes and air as coolant fluid in the heat sinks.

REFERENCES

[1] A. Rezania, K. Yazawa, L.A. Rosendahl, A. Shakouri, Co-optimized design of microchannel heat exchangers and thermoelectric generators, International Journal of Thermal Sciences 72 (2013) 73-81.

[2] N. Wojtas, L. Rüthemann, W. Glatz, C. Hierold, Optimized thermal coupling of micro thermoelectric generators for improved output performance, Renewable Energy 60 (2013) 746-753.

[3] A. Rezania, L.A. Rosendahl, H. Yin, Parametric optimization of thermoelectric elements footprint for maximum power generation, Journal of Power Sources 255 (2014) 151-156.

[4] T.J. Hendricks, Thermal system interactions in optimizing advanced thermoelectric energy recovery systems, Journal of Energy Resources Technology 129 (2007) 223-231.

[5] X.F. Zheng, C.X. Liu, R. Boukhanouf, Y.Y. Yan, W.Z. Li, Experimental study of a domestic thermoelectric cogeneration system, Applied Thermal Engineering 62 (2014) 69-79.

[6] Ercan M. Dede, Yan Liu, Experimental and numerical investigation of a multi-pass branching microchannel heat sink, Applied Thermal Engineering 55 (2013) 51-60.

[7] M. Reyes, J.R. Arias, A. Velazquez, J.M. Vega, Experimental study of heat transfer and pressure drop in micro-channel based heat sinks with tip clearance, Applied Thermal Engineering 31 (2011) 887-893.

[8] A. Rezania, L.A. Rosendahl, S.J. Andreasen, Experimental investigation of thermoelectric power generation versus coolant pumping power in a microchannel heat sink, International Communications in Heat and Mass Transfer 39 (2012) 1054-1058.

[9] P. Gunnasegaran, H.A. Mohammed, N.H. Shuaib, R. Saidur, The effect of geometrical parameters on heat transfer characteristics of microchannels heat sink with different shapes, Int. J. Heat and Mass Transfer 37 (2010) 1078–1086
[10] D.B. Tuckerman, R.F.W. Pease, High-performance heat sinking for VLSI, IEEE Electron Device Letters 2 (1981) 126–129.
[11] J.Y. Jang, Y.C. Tsai, C.W. Wu, A study of 3-D numerical simulation and comparison with experimental results on turbulent flow of venting flue gas using thermoelectric generator modules and plate fin heat sink, Energy 53 (2013) 270-281.
[12] E.E. Antonova, D.C. Looman, Finite elements for thermoelectric device analysis in ANSYS, 24th International Conference on Thermoelectrics (2005) 215- 218.
[13] M. Chen, L.A. Rosendahl, T. Condra, A three-dimensional numerical model of thermoelectric generators in fluid power systems, International Journal of Heat Mass Transfer 54 (2011) 345-355.
[14] R.A. Serway, Principles of Physics, 2nd ed., Fort Worth, Texas; London: Saunders College Publishing (1998) 602.
[15] M.I. Hasan, Investigation of flow and heat transfer characteristics in micro pin fin heat sink with nanofluid, Applied Thermal Engineering 63 (2014) 598-607.
[16] Y. Chen, C. Zhang, M. Shi, J. Wu, Three-dimensional numerical simulation of heat and fluid flow in noncircular microchannel heat sinks, International Communications in Heat and Mass Transfer 36 (2009) 917-920.